Project	**IEEE 802.16 Broadband Wireless Access Working Group <http://ieee802.org/16>**
Title	**Multipath Measurements and Modeling for Fixed Broadband Point-to-Multipoint Radio wave Propagation Links under different Weather Conditions**
Date Submitted	**2000-02-25**
Source	Hao Xu[†] Prof. Theodore S. Rappaport[†] Vikas Kukshya[†] Hossein Izadpanah[††] [†]The Bradley Dept. of Electrical and Computer Engineering, 432 NEB, MPRG, Virginia Tech, Blacksburg, VA 24061 [††]HRL Laboratories, 3011 Malibu Canyon Road, Malibu, CA Voice: +1 540 2312919 Fax: +1 540 2312968 mailto:wireless@vt.edu
Re:	This contribution is in response to IEEE 802.16 PHY Task Group Call for Contributions on Modeling Issues, Jan. 23, 2000
Abstract	This submission concisely presents analysis of the mm-wave broadband channel propagation data collected under different weather conditions. The emphasis is on measurement based propagation models for small scale fading in rain, for average rain attenuation and large-scale attenuation over broadband millimeter wave links. A deterministic modeling technique for link design is also presented.
Purpose	The purpose of this contribution is to propose guidelines for the design of models for broadband wireless channels and thereby facilitate the PHY Task Group's efforts at standardization.
Notice	This document has been prepared to assist the IEEE 802.16. It is offered as a basis for discussion and is not binding on the contributing individual(s) or organization(s). The material in this document is subject to change in form and content after further study. The contributor(s) reserve(s) the right to add, amend or withdraw material contained herein.
Release	The contributor acknowledges and accepts that this contribution may be made public by 802.16.
IEEE Patent Policy	The contributor is familiar with the IEEE Patent Policy, which is set forth in the IEEE-SA Standards Board Bylaws <http://standards.ieee.org/guides/bylaws> and includes the statement: "IEEE standards may include the known use of patent(s), including patent applications, if there is technical justification in the opinion of the standards-developing committee and provided the IEEE receives assurance from the patent holder that it will license applicants under reasonable terms and conditions for the purpose of implementing the standard." See <http://ieee802.org/16/ipr> for details.

Multipath Measurements and Modeling for Fixed Broadband Point-to-Multipoint Radiowave Propagation Links under different Weather Conditions

Hao Xu[†], Theodore S. Rappaport[†], Vikas Kukshya[†], Hossein Izadpanah[††]

[†]Mobile and Portable Radio Research Group
Bradley Department of Electrical and Computer Engineering
Virginia Polytechnic Institute and State University, Blacksburg, VA 24061
Tel: (540) 2312927, Email: wireless @vt.edu

[††]HRL Laboratories, 3011 Malibu Canyon Road, Malibu, CA

1. Introduction

Thorough knowledge of a millimeter wave wideband channel is essential to determine the combination of modulation, diversity, equalization and coding required for optimizing the channel capacity and bit error performance. Proper channel models are also vital for deployment with proper link margins. It is therefore necessary to study degrading propagation phenomena such as reflection, diffraction and scattering extensively to be able to design and deploy efficient communication links. However at frequencies above 10GHz, not only must one consider propagation phenomena mentioned above, but also the interaction of electromagnetic waves with atmosphere and particles such as rain, snow and hail [1][2].

This contribution provides detailed analysis of high-resolution wideband (200MHz RF bandwidth) 38GHz propagation measurements under different weather conditions over link lengths of 200 to 600 meters. The paper places emphasis on models based on measurements for these broadband links. Specifically, it presents measurement based propagation models for small-scale fading and large-scale attenuation of millimeter wave links due to average rain attenuation. A fast, deterministic modeling technique for link design is also derived and presented. The data correlation analysis and modeling are based on a measurement campaign conducted at Virginia Tech via three cross-campus links from April to June 1998. An unobstructed, a partially obstructed and a completely obstructed LOS link were selected to represent typical LMDS micro/pico scenarios.

2. Measurement System Hardware and Link Setup [3]

To recreate a typical LMDS link, a sector horn transmitting antenna and a parabolic reflector-receiving antenna were used during the measurements. A *spread spectrum sliding correlator channel sounder* [4] was used to record the Power Delay Profiles (PDPs). The channel sounder uses an intermediate frequency of 5.4 GHz that is up-converted to an RF output of 37.8 GHz. High precision Rubidium oscillators were used to drive both the pseudonoise (PN) sequence generators and the IF clocks. The PN clock was set to 100 MHz to achieve a time resolution of 10ns and a null-to-null RF Bandwidth of 200 MHz. With appropriate settings, the system recorded as many as 50 PDPs per second. At each measurement site, received CW power levels were recorded every hour to verify the system stability. System hardware performance was verified by performing Free Space calibration during clear weather conditions.

Rain rates were measured every minute using a tipping bucket rain gauge with a resolution of 15.24mm/hr. Also, weather data files and measured channel responses were time stamped to establish a one-to-one correspondence between the channel PDP measurements and the recorded weather conditions.

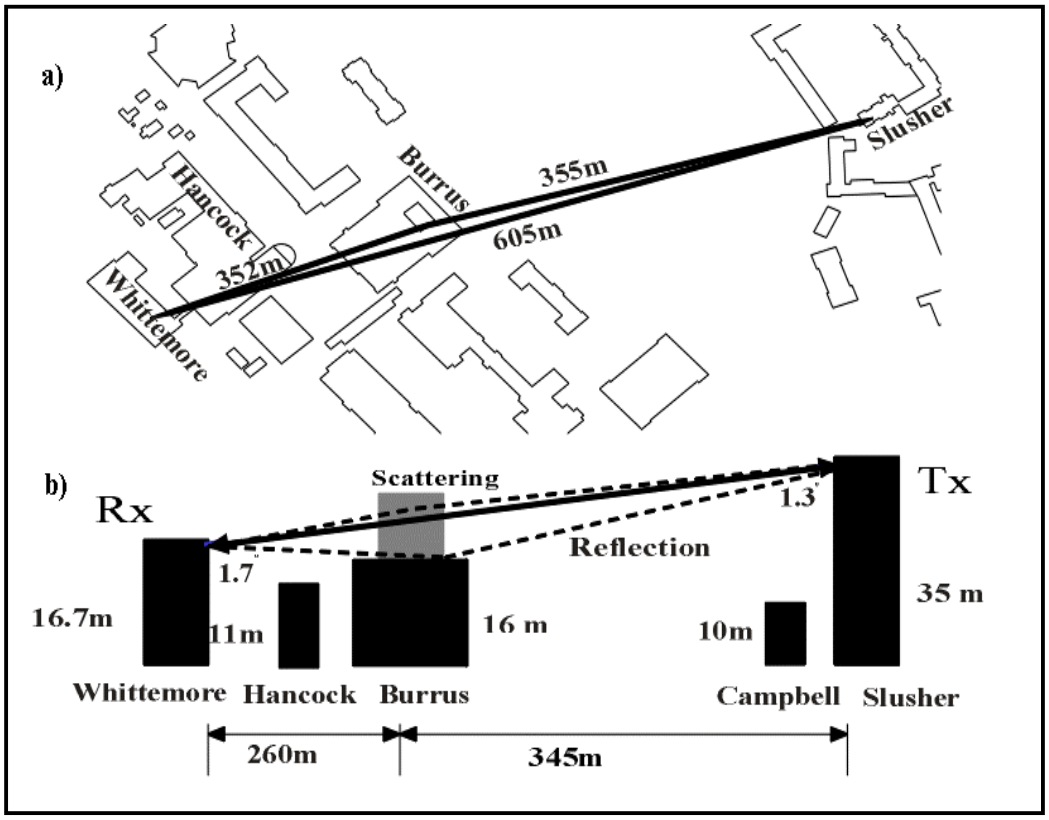

Figure 1. Slusher-Whittemore Link: 605 m unobstructed LOS Link (**L1**) (a) Top View (b) Side View

Table 1 lists the particulars about three cross-campus point-to-point links. Their geometry is shown in Figure 1 and Figure 2. The first link, L1, provided an unobstructed LOS path. The second link, L2, provided a path obstructed by the dense canopy of a big oak tree. The third link, L3, provided a partially obstructed path, where the leaves of an oak tree were sufficiently close to the LOS path and would partially obstruct the LOS path during windy weather conditions. For all PDP measurements, the transmitter and the receiver were both located indoors and were left to run continuously to maintain antenna alignment, constant gain and to capture sudden weather changes.

TABLE 1 Relevant parameters for wideband Point-to-Point Links

Locations	T-R (m)	H*(Tx) (m)	H*(Rx) (m)	Clearance
L1: Slusher – Whittemore	605	663	645	Unobstructed LOS
L2: McBryde – Student Center (GBJ)	265	652	637	Entirely obstructed LOS
L3: McBryde – Student Center (GBJ)	265	652	637	Partially obstructed LOS

***** The heights of Tx and Rx are with respect to sea level.

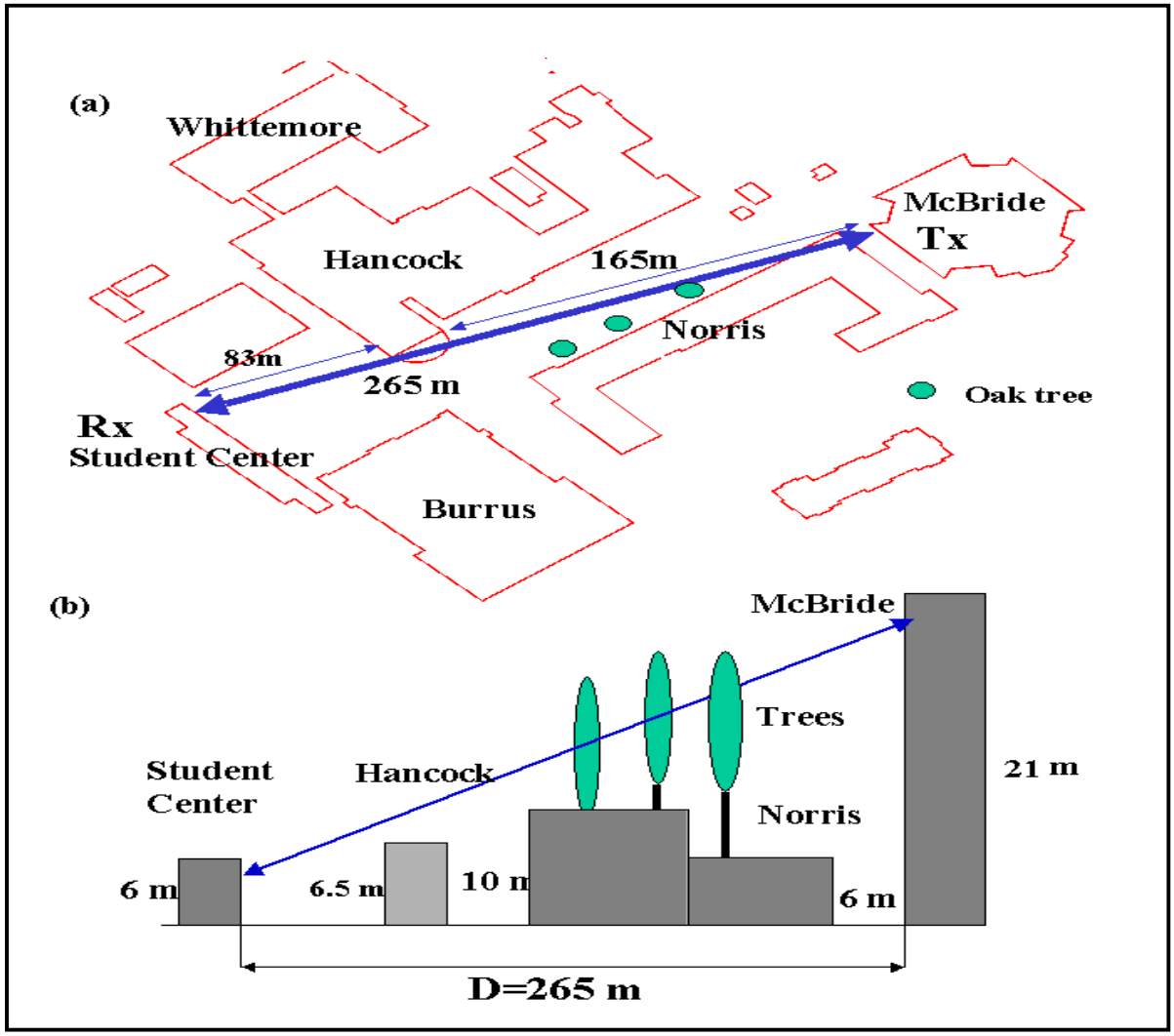

Figure 2 Geometry of the McBryde Student Center Links: 265 m obstructed LOS Link (**L2**) and partially obstructed LOS Link (**L3**). (a) Top View (b) Side View

3. Measurement Results and Statistical Channel Models [3]

As many as 73,963 PDPs were recorded for the three cross-campus links for different weather conditions. Each PDP was independently processed to determine the number of multipath components above a noise threshold, LOS power, excess delay time, the mean excess delay and the RMS spread.

Since the specular reflected wave gets considerably reduced due to the rough surface scattering, and the reflected waves with large Angle of Arrival (AOA) are rejected by highly directional antennas, there was no multipath observed on the link L1 (unobstructed LOS) under clear weather conditions. However, multipath components were detected on the L1 link during rain and hail. As expected, strong multipath components (only 9dB below LOS component) were detected in as many as 30 PDPs for obstructed LOS links L2 and L3 during rain and hail events. The results confirmed that severe weather conditions and vegetation cause multipath.

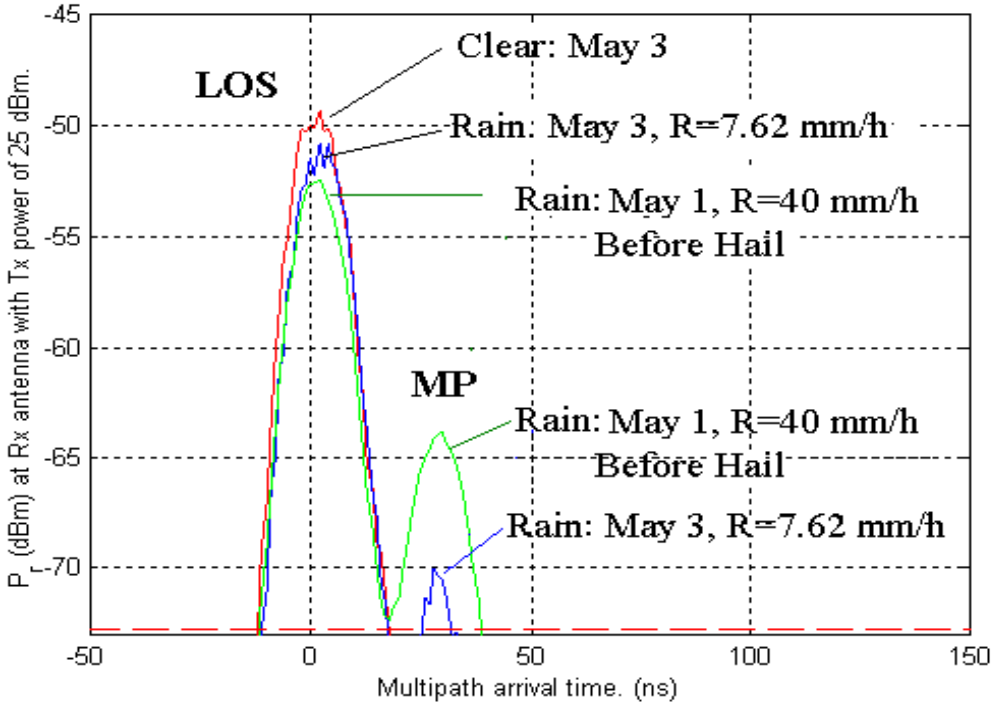

Figure 3. Comparison of PDPs under different weather conditions: 605 m unobstructed LOS link [5]

3.1 Model for Small Scale Fading in Rain

The measurement speed of 50 PDPs per second allows the measurement system to record huge volumes of data within a short period of time and hence track the channel dynamics. Results from Figure 3 show a wide variation of the received signal power at constant rain rates.

During rain, the received signal can be modeled as the sum of a constant (coherent) component and randomly scattered (incoherent) components resulting from rain or other scatteres. The resulting signal is therefore expected to follow a Rician Distribution.

The Rician probability density function (pdf) for the received signal envelope, $f_V(v)$, is [6]

$$f_V(v) = \frac{v}{\sigma^2}\exp\{-\frac{v^2 + A^2}{2\sigma^2}\}Io(\frac{Av}{\sigma^2}) \quad (1)$$

where v is the signal envelope, $A^2/2$ is the coherent power, σ^2 is the incoherent power and $I_o(\cdot)$ is the modified Bessel function of the first kind and zero order.

The Rician pdf is typically used to model the received envelope in a wireless channel that has a LOS. The pdf for the received power, $P = V^2/2$, is then given by

$$f_P(p) = \frac{1}{\sigma^2}\exp\{-\frac{2p + A^2}{2\sigma^2}\}Io(\frac{A\sqrt{2p}}{\sigma^2}) \quad (2)$$

where p is the random variable of the received power.

Histograms of the received power at constant rain rate over short periods of 1-2 minutes are well described by (2). An example of measured and theoretical pdf from (2) is shown in Figure 4(a).

Also, the Rician parameters A and σ, can be calculated from the mean and standard deviation of the received power from the measured data. By definition, the mean received power, μ_p, and standard deviation σ_p^2 are given by

$$\mu_p = \mathrm{E}\{p\} = \int_0^\infty p f_p(p)dp = \sigma^2 + A^2/2 \quad (3)$$

$$E\{p^2\} = \int_0^\infty p^2 f_p(p)dp = 2\sigma^4 + 2A^2\sigma^2 + A^4/4 \quad (4)$$

$$\sigma_p = E\{p^2\} - E^2\{p\} = \sigma^4 + A^2\sigma^2 \quad (5)$$

where E{} denotes ensemble average. Rician parameters A and σ, can be calculated from (3) and (5).

Rician distribution can also be parameterized by total power and the K factor, which is defined as the ratio of coherent to incoherent powers in dB. Using μ_p and σ_p from (3) and (5), K is computed as follows (in dB)

$$K = 10\log_{10}\frac{A^2/2}{\sigma^2} = 10\log_{10}\frac{\sqrt{\mu_p^2 - \sigma_p^2}}{\mu_p - \sqrt{\mu_p^2 - \sigma_p^2}} \quad (6)$$

Equation (6) shows that the K factor is independent of the total received power. The received power is therefore normalized before calculating K. The resulting K factors for different rain rates are presented in Figure 4(b).

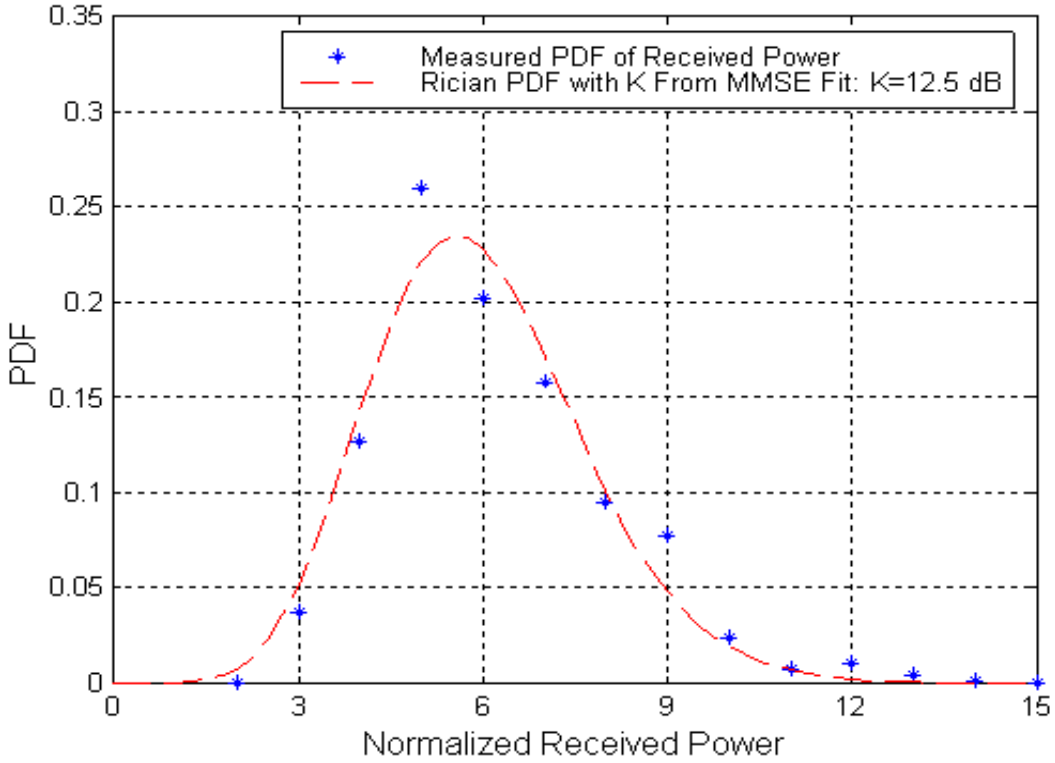

Figure 4(a) Short term variation of Received power at rain rate of 122 mm/hr.

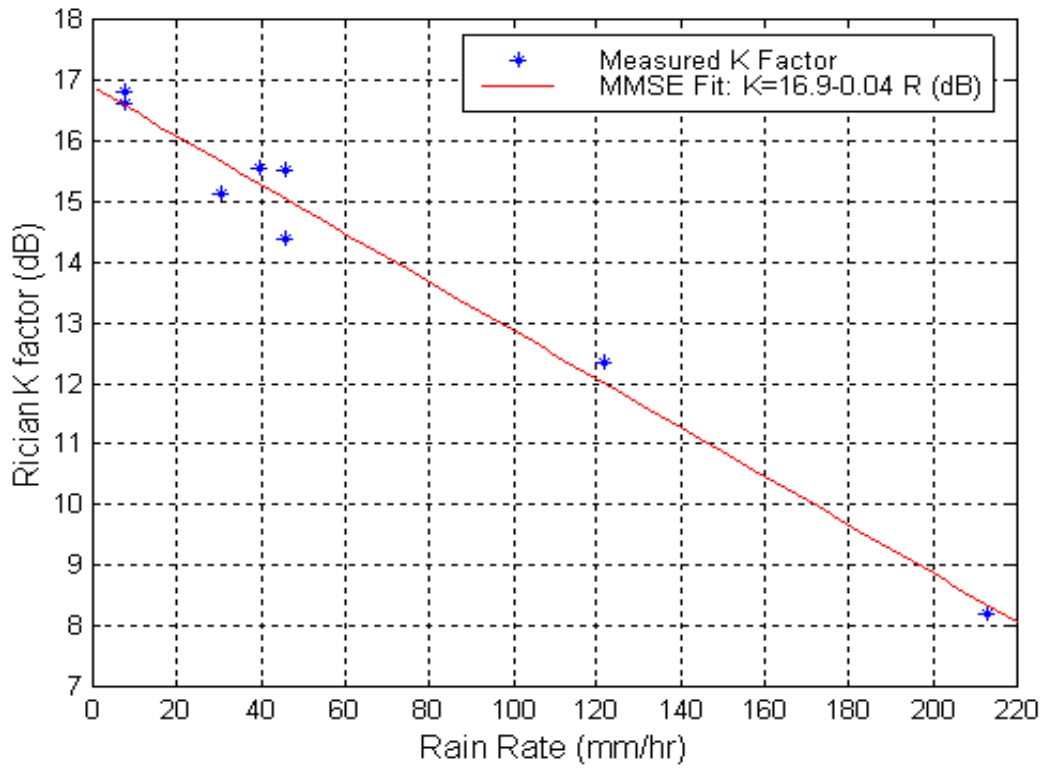

Figure 4(b) Rician K factor vs. Rain rate

Rain Attenuation Distribution on 265m partially obstructed LOS link, Rain rate of 122mm/hr [3]

A Minimum Mean Square Error (MMSE) fit is applied to the data, which leads to the following relationship between the Rician K factor (dB) and rain rate R (mm/hr):

$$K = 16.88 - 0.04R \text{ dB} \quad (7)$$

Equation (7) shows that the K factor is proportional to Rain rate (R). This is expected because with an increase in rain rate, coherent power decreases and incoherent scattered power increases. The PDPs indeed (Figure 3) show a decrease of the LOS power as the multipath power increases during rain.

Equation (7), combined with the received total power estimate, provides a powerful tool to model received signal variation and the resultant outage probability for LMDS systems. For a given rain rate and path length, the total received power can be estimated from (11) and (12) and K factor can be determined by (7).

3.2 Model for Average Rain Attenuation

The plot of measured Rain Attenuation vs. the Rain Rate (Figure 5) is drawn out of the PDPs recorded during a heavy rainstorm. At a rain rate of 213mm/hr, the rain attenuation was as high as 26 dB. As expected, the received signal power displays a strong correlation with rain rate. Figure 6 provides a summary of average rain attenuation vs. rain rate.

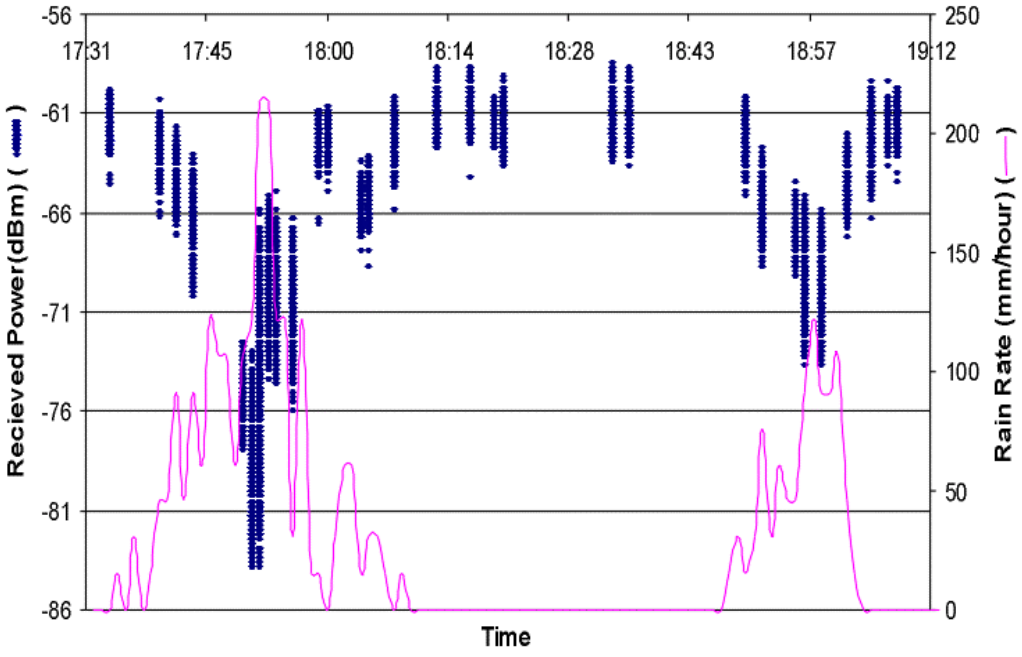

Figure 5. Rain Attenuation Measurements: June 2, 265 m Partially Obstructed LOS

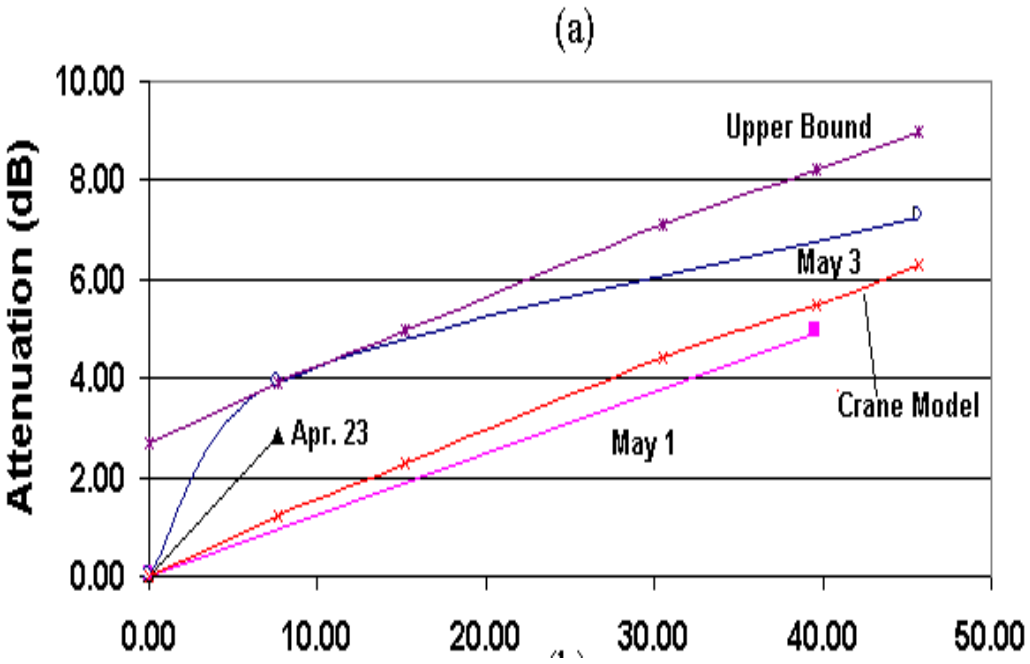

Figure 6(a) Rain Attenuation Summary and Upper Bounds for 605m unobstructed

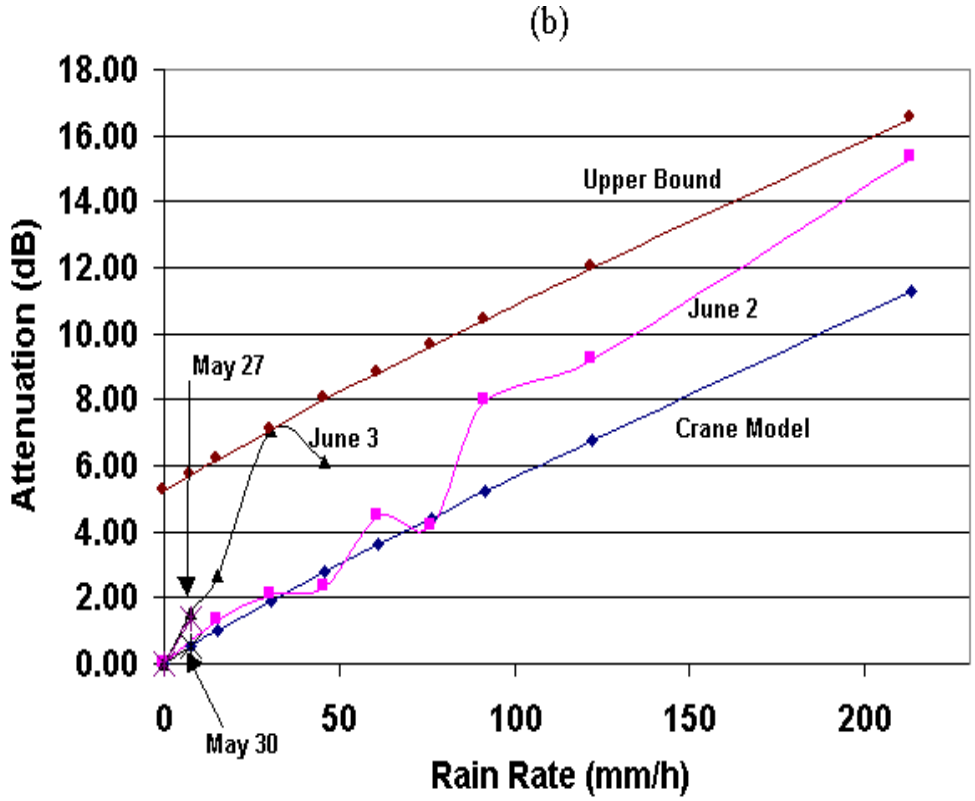

Figure 6(b) Upper Bounds for 265m partially obstructed and obstructed LOS links

The Crane Model is a theoretical prediction model based on the geophysical observations of rain rate, rain structure, and the vertical variation of atmosphere temperature. The model is summarized in equation (8) through (10) [2]

$$A_R = aR^b[\frac{e^{ubd}-1}{ub}] \qquad \text{(for } 0 \le D \le d\text{)} \qquad (8)$$

$$A_R = aR^b[\frac{e^{ubd}-1}{ub} - \frac{B^b e^{cbd}}{cb} + \frac{B^b e^{cbD}}{cb}] \qquad \text{(for } d \le D \le 22.5\text{km)} \qquad (9)$$

where

$$u = \ln[B\, e^{cd}]/d\ ; \quad B = 2.3\, R^{-0.17}\ ; \quad c = 0.026 - 0.03 \ln(R)\ ; \quad d = 3.8 - 0.6 \ln(R)\ \text{km} \qquad (10)$$

and A_R is path attenuation due to rain in dB, R is point rain rate in mm/hr and D is path length in km. For paths longer than 22.5 kms, the attenuation A_R is calculated for a 22.5-km path and the resulting rain outage time is multiplied by a factor of (D/22.5). Multipliers a and b are rain attenuation coefficients dependent on frequency and polarization.

Example of Crane Model Calculation

In Virginia, for example, the rain climate is D2 [2]. For vertical polarization, at 38 GHz, the coefficients a and b are 0.28 and 0.943 respectively. From the point rain rate vs. time distribution table, the rain rate is 49.0 mm/hr. For this rain rate, from Equation (10), we get B = 1.187, c = -0.0908 and d = 1.4649kms.

For path lengths of 206 m and 605 m, the predicted rain attenuation can be calculated using Equation (8) as

$$A_R = (0.281)(49)^{0.943}[(e^{ubd} - 1)/(ub)]$$

The calculated values come out to be 2.3 dB and 6.7 dB for link lengths of 206 and 605 m respectively.

As shown in Figure 6, the measurement results show slightly higher attenuation than the Crane Model prediction. For unobstructed LOS Link L1, the difference between the Crane Model and measurements is within 2.7 dB. This difference is as high as 5.2 dB for obstructed links L2 and L3.

The upper bounds for rain attenuation calculated from measurements for LOS and obstructed LOS links can be respectively given as

$$P_{LOS}(R, D) = P_{crane}(R, D) + 2.7\ (\text{dB}) \qquad (11)$$

$$P_{Partial\ LOS}(R, D) = P_{crane}(R, D) + 5.2\ (\text{dB}) \qquad (12)$$

where P_{crane} is the attenuation estimate based on the Crane model, R(mm/hr) is the rain rate and D(m) is the path length. The upper bound for partially obstructed LOS path provides an attenuation estimate that accounts for both rain and foliage.

4. Geometrically based Multipath Channel Models [7]

4.1 General Description of the Model

A method to predict multipath channel characteristics based on a two-dimensional geometrical LOS model with Omni-directional antenna is given in [8]. The model developed in this work is a generalized three-dimensional model appropriate for any antenna. The model has been devised to predict the maximum multipath delay or maximum multipath power that could arise in a LMDS link.

The geometry of the model is depicted in Figure 7. The LOS path length is D, and a scatterer is assumed to be located at (x_0, y_0, z_0). The scatterer may be any object that has a large reflecting surface relative to the wavelength. When highly directional antennas are used, only scatterers that are sufficiently close to the LOS path cause strong multi-paths. For worst-case scenario appropriate for equalizer design specification, each scatterer is assumed to be a perfect reflector with a reflection coefficient of unity.

Under the assumption that the scatterer is a large perfect reflector, the relative received power, ΔP_{MP}, and excess delay time, τ_{MP}, of each multipath component are computed as shown.

$$\tau_{MP} = (d_1 + d_2 - D)/c \tag{13}$$

$$\Delta P_{MP} = G_t(\phi_t, \theta_t) + G_r(\phi_r, \theta_r) - (PL(d_1 + d_2) - PL(D)) \tag{14}$$

where d_1 and d_2 are the distances from the reflector to the transmitter and the receiver, c is the speed of light and G_t and G_r are normalized antenna power patterns for transmitter and receiver.

The term $(PL(d_1+d_2)-PL(D))$ is the excess free space path loss associated with the path length difference between the reflected path and the LOS path. The parameters ΔP_{MP} and τ_{MP} are calculated in dB and seconds respectively. For a given path length D and the location of the reflector (x_0, y_0, z_0), all the other parameters can be determined from the geometry of Figure 7.

The model is demonstrated for following canonical antenna system: the uniformly illuminated rectangular aperture antenna used as the transmitting antenna and the uniformly illuminated circular aperture antenna used as the receiving antenna.

The normalized far field radiation power patterns for these antennas are given in [9] as follows

$$G_t(\phi_t, \theta_t) = \left| \frac{\sin[\pi(a/\lambda)\sin(\phi)]\sin[\pi(b/\lambda)\sin(\theta)]}{\pi^2(ab/\lambda^2)\sin(\phi)\sin(\theta)} \right|^2 \tag{15}$$

where λ is the wavelength and a,b are the dimensions of the rectangular aperture.

$$G_r(\gamma_r) = \left| \pi r^2 2J_1(\xi)/\xi \right|^2 \tag{16}$$

where $\xi = 2\pi(r_0/\lambda)\sin(\gamma_r)$, J_1 is the first order Bessel function, and γ_r is the angle in the spherical coordinate system as shown in Figure 7.

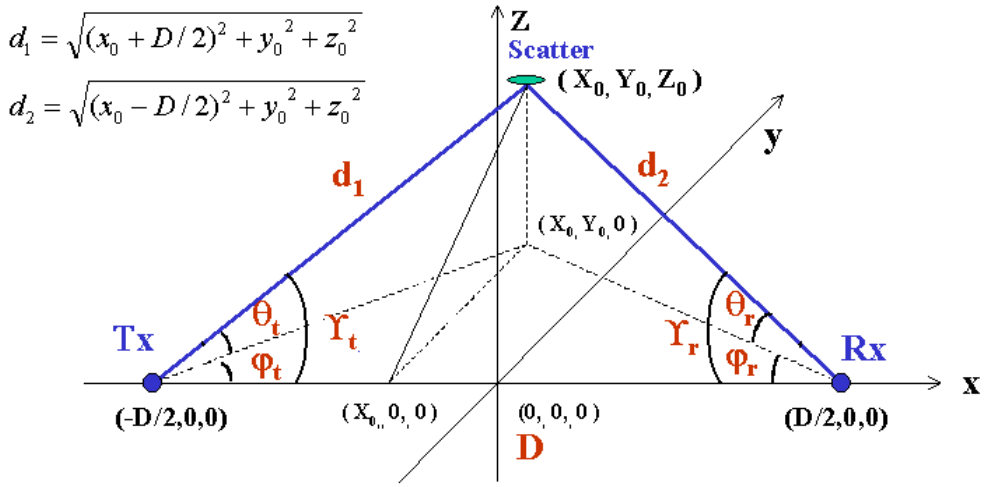

$$d_1 = \sqrt{(x_0 + D/2)^2 + y_0^2 + z_0^2}$$

$$d_2 = \sqrt{(x_0 - D/2)^2 + y_0^2 + z_0^2}$$

$$\phi_t = \sin^{-1}\frac{y_0}{\sqrt{(x_0 + D/2)^2 + y_0^2}} \qquad \phi_r = \sin^{-1}\frac{y_0}{\sqrt{(x_0 - D/2)^2 + y_0^2}}$$

$$\theta_t = \sin^{-1}\frac{z_0}{d_1} \qquad \gamma_t = \sin^{-1}\frac{\sqrt{y_0^2 + z_0^2}}{d_1} \qquad \theta_r = \sin^{-1}\frac{z_0}{d_2} \qquad \gamma_r = \sin^{-1}\frac{\sqrt{y_0^2 + z_0^2}}{d_2}$$

Figure 7 Geometry of the Model – On a three dimensional axis, (x_0, y_0, z_0) represents the position of the scaterrer and 'D' is the distance of separation between the Transmitter and Receiver. Distances 'd1' and 'd2' represent distances between the scaterrer and the transmitter & receiver respectively.

4.2 Relative Power Zone and Excess Delay Zone

We define the *relative power zone* as the region where a perfect reflector (with Γ = 1) would give rise to a multipath component whose power is within a certain range relative to the LOS component. Similarly, we define the *excess delay zone* as the region where a perfect reflector would give rise to a multipath component whose excess propagation delay is within a certain range of delay relative to that of the LOS component.

For a general excess delay $\tau_{MP,}$ the boundary of the excess delay zone given by (13) is an ellipsoid and the closed form equation for the ellipsoid is

$$\frac{x_0^2}{K_t^2/4} + \frac{y_0^2}{K_t^2/4 - D^2/4} + \frac{z_0^2}{K_t^2/4 - D^2/4} = 1 \qquad (17)$$

where $K_t = D + (c)(\tau_{MP})$ is a constant. An example of the excess delay zones is depicted in Figure 8. The contours represent excess delay zone boundaries.

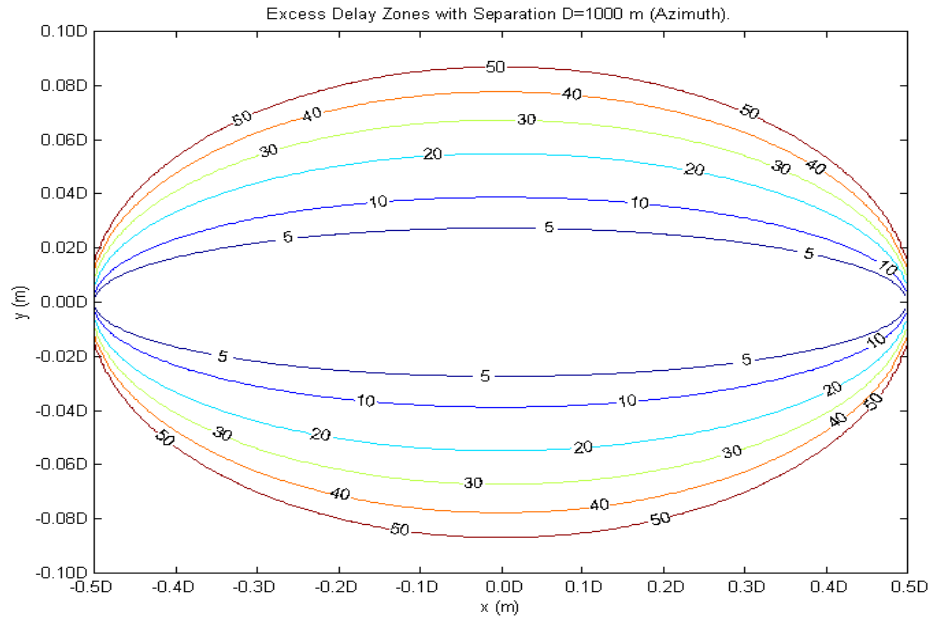

Figure 8. Excess Delay Contour Plot D = 1000m, Azimuth Plane, Γ = 1, all units

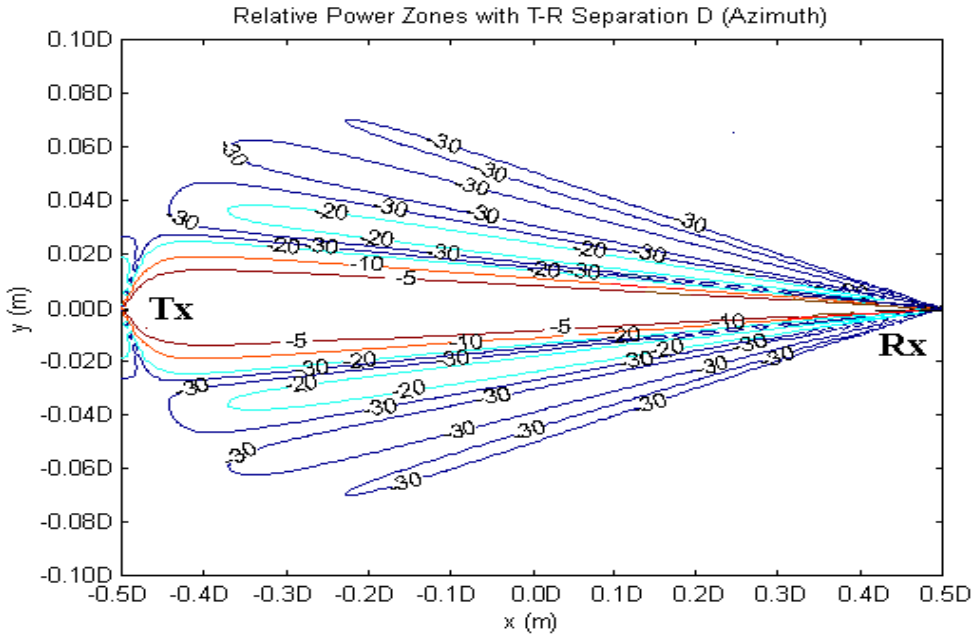

Figure 9. Relative Power Contour Plot Horn and Parabolic Antennas, Azimuth Plane, Γ = 1, all units

In the same way, for a given relative power level ΔP_{MP}, the relative power zone can be calculated using (14). The resulting relative power zones for the canonical antennas are presented in Figure 9, where the contours represent the power zone boundaries. These plots can be used to effectively identify worst-case multipath statistics for any millimeter wave point-to-point deployment. Delay and Power of multipath components can be easily estimated by overlaying the plots onto a site map.

Expected delay τ_{MP}, expected power ΔP_{MP} and LOS path length D can be used to analytically determine maximum radii of excess delay zone and relative power zone. From (17), maximum radius of an excess delay zone, y_{dz}^{max} is given by the following relationship.

$$y_{dz}^{max} = \sqrt{K_t^2/4 - D^2/4} \qquad (18)$$

where $K_t = D + (c)(\tau_{MP})$. Similarly the maximum radii of relative power zone y_{pz}^{max} can be evaluated using (14). The results are shown in Table 2.

TABLE 2 Maximum radii of relative power zone and excess delay zone for horn and parabolic antennas

D(m)	Max. Relative Power Zone radii (m)				
ΔP_{MP}	5dB	10dB	20dB	30dB	35dB
500	7	10	19	35	46
1000	14.5	19.5	38.5	70	92
2000	29	39	77	140	185
5000	72	96	192	352	461

D(m)	Max. Excess Delay Zone radii (m)				
τ_{MP}	10ns	20ns	30ns	40ns	50ns
500	27.4	38.8	47.6	55.1	61.7
1000	38.8	54.9	67.2	77.7	86.9
2000	54.8	77.5	95.0	109.7	122.7
3000	67.1	94.9	116.3	134.3	150.2
4000	77.5	109.6	134.2	155.0	173.4
5000	86.6	122.5	150.1	173.3	193.8

However, the exact relationship between maximum radii of relative power zone, y_{pz}^{max} and ΔP_{MP} requires solution of Bessel function and sinc function from (15) and (16). A polynomial fit can be applied to the results from Table 2 to obtain an intermediate expression as below

$$y_{pz}^{max} = \frac{D}{1000}(0.07\Delta P_{MP}^2 - 0.1947\Delta P_{MP} + 12.6311) \qquad (19)$$

Equation (18) and (19) provide closed form estimates of the worst-case delay and power of multipath from a scatterer and can greatly simplify LMDS site planning and deployment.

5. Conclusions

This contribution presents the results of a wideband measurement campaign performed on three point-to-point links at 38 GHz. The purpose of the research was to study the effects of various weather events such as rain and hail on the behavior of broadband millimeter wave channel. The measurement campaign was performed at 38 GHz on a 605m unobstructed link, a 265m obstructed link and a 265m partially obstructed link. A total of 73,963 PDPs were recorded under clear, rain and hail conditions.

Weather effects on received signal power were analyzed in terms of *mean attenuation* and *short-term variation.* Short-term signal variation was analyzed for 1-2 minute intervals at constant rain rates. Results show that the received signal variation follows a Rician distribution.

Upper bounds of the mean attenuation were provided based on a modified Crane model for both unobstructed and partially obstructed LOS links as functions of rain rate and path length.

Finally, a fast deterministic approach was developed to facilitate estimation of multipath power, TOA and AOA in a LOS millimeter wave system. Relative Power Zones and Excess Delay Zones are defined to predict multipath power and arrival time. Since these contour plots and zone boundaries are dependent only on the antenna patterns and the link length, they may be easily mapped onto any site. Potential reflectors can be quickly determined by simply overlaying the contour plots on the site map.

References

1. R.L.Freeman, *Radio System Design for Telecommunications (1-100GHz).* New York: John Wiley & Sons, 1987.
2. R.K.Crane, *Electromagnetic Wave Propagation through Rain.* New York: John Wiley & Sons, 1996.
3. H.Xu, T.S. Rappaport, R. J. Boyle, and J. Schaffner, "Measurements and Models for 38 GHz Point-to-Multipoint Radiowave Propagation" accepted to *IEEE Journal on Selected Area of Communications*, March 2000
4. H. Xu, T. S. Rappaport, J. H. Schaffner, and H. P. Hsu. "The Sliding Correlator and Network Analyzer Channel Sounding Methods for Wideband Multipath Propagation Measurements at 5.85 GHz," *Advancing Microelectronics: Special Wireless Issue*, vol. 25, no. 3, pp. 40-54, 1998.
5. H. Xu, T. S. Rappaport, R. J. Boyle, J. H. Schaffner, "38 GHz Wideband Point-to-Multipoint Measurements under Different Weather Conditions," IEEE Communications Letters, Vol. 4, No. 1, January 2000, pp. 7-8.
6. S.O.Rice, "Statistical Properties of a Sine Wave Plus Random Noise," in *Bell System Technical Journal*, vol. 27, pp. 109-157, Jan.1948.
7. H.Xu, T.S.Rappaport, R.J.Boyle and J.H.Schaffner, "38GHz Wideband Point-to-Multipoint Radio Wave Propagation Study for a Campus Environment" in *Proc. IEEE VTC'99*, May 1999..
8. J.Liberti and T.S.Rappaport, "A Geometrically Based Model for Line of Sight Multipath Radio Channels," in *Proc. IEEE VTC'96*, (Atlanta, GA), pp.844-848, Apr. 1996.
9. M.Skolnik, *Introduction to Radar Systems.* New York: McGraw-Hill, 2nd edition, 1980.